Agricultural Water Management xxx (2015) xxx–xxx

Contents lists available at ScienceDirect

Agricultural Water Management

journal homepage: www.elsevier.com/locate/agwat

Optimizing conjunctive use of surface water and groundwater for irrigation to address human-nature water conflicts: A surrogate modeling approach

Xin Wu [a], Yi Zheng [a,*], Bin Wu [a], Yong Tian [a,b], Feng Han [a,b], Chunmiao Zheng [a,b,c]

[a] College of Engineering, Peking University, Beijing 100871, China
[b] School of Environmental Science and Engineering, South University of Science and Technology, Shenzhen 518055, Guangdong Province, China
[c] Department of Geological Sciences, University of Alabama, Tuscaloosa, Alabama, United States

ARTICLE INFO

Article history:
Received 6 February 2015
Received in revised form 16 July 2015
Accepted 26 August 2015
Available online xxx

Keywords:
Irrigation
Water diversion
Integrated surface water–groundwater modeling
Surrogate modeling
Optimization
Heihe River Basin

ABSTRACT

In arid and semi-arid areas where agriculture competes keenly with ecosystem for water, integrated management of both surface water (SW) and groundwater (GW) resources at a basin scale is crucial, but often lacks scientific support. This study implemented physically-based, fully integrated SW–GW modeling in optimizing water management, and performed surrogate modeling to replace the computationally expensive model with simple response surfaces. Water use conflicts between agriculture and ecosystem in Heihe River Basin (HRB), the second largest inland river basin in China, were investigated. Based on the integrated model GSFLOW (Coupled Ground-Water and Surface-Water Flow Model), the conjunctive use of SW and GW for irrigation in the study area was optimized using a surrogate-based approach named DYCORS (DYnamic COordinate search using Response Surface models). Overall, the study demonstrated that, with the surrogate modeling approach, an expensive integrated model could be efficiently incorporated into an optimization analysis, and the integrated modeling would make feasible a physically based interpretation of the optimization results. In the HRB case study, the surrogate-based optimization suggested a very different time schedule of water diversion in opposite to the existing one, indicating the critical role of SW–GW interactions in the water cycle. With the temporal optimization, a basin-scale water saving could be achieved by reducing non-beneficial evapotranspiration. In addition, the current flow regulation in HRB may not be sustainable, because the ecosystem recovery in the lower HRB would be at the cost of the ecosystem degradation in the middle HRB.

1. Introduction

In many arid and semi-arid inland river basins, irrigated farmlands compete keenly with the regional ecosystem for scarce water resources (Krebs et al., 1999; Wichelns and Oster, 2006). Typically, the temporal mismatch between river flow and irrigation water demand is notable in such areas, and flow conservation for natural ecosystem is an important management concern. In areas where surface water (SW) and groundwater (GW) strongly interact, aquifers could behavior like “reservoirs”, with which the temporal mismatch and/or the human-nature competition may be alleviated (Forrester and Keane, 2009; Simons et al., 2015; Singh, 2014a). In water-limited environments, groundwater pumping in addition to surface water diversion for irrigation is a common practice (Cosgrove and Johnson, 2005; Liu et al., 2010; Singh, 2014a; Smout and Gorantiwar, 2005), and optimizing the conjunctive use of SW and GW is an important research topic for agricultural water management (Bouwer, 2002; Khare et al., 2006; Kumar et al., 2013; Safavi and Esmikhani, 2013; Singh, 2014b).

Simulation-optimization (SO) approaches are widely used in water resources management and planning, which couple hydrologic or hydro-agronomic modeling with mathematical optimization (Singh, 2014a,b). They have been applied to address different irrigation water management issues, such as improving crop productivity by optimizing land and water allocation (Khare et al., 2006; Smout and Gorantiwar, 2005; Singh and Panda, 2012), altering Best Management Practices (BMPs) to adapt to climate change (Cai et al., 2015), assessing optimal locations and pumping rates in coastal aquifers to avoid saltwater intrusion (Bhattacharjya and Datta, 2005; Mantoglou and Papantoniou, 2008; Reichard and Johnson, 2005), and controlling non-point pollution of agriculture (Tan et al., 2011). SO has been implemented to the issue of con-

* Corresponding author: Fax: +86 18618126436.
E-mail address: yizheng@pku.edu.cn (Y. Zheng).

http://dx.doi.org/10.1016/j.agwat.2015.08.022
0378-3774/

junctive use of SW and GW as well (Safavi and Esmikhani, 2013; Singh, 2014b; Singh and Panda, 2013; Tabari and Soltani, 2012). However, to avoid the tremendous computational cost, most of the studies adopted hydrological simulation with no detailed discription of SW–GW interactions. Some optimization studies involved the 3-D groundwater flow model MODFLOW (Chang et al., 2010; Harbaugh, 2005; Safavi and Esmikhani, 2013), but the groundwater recharge processes are highly simplified in MODFLOW. The widely used SWAT model (Arnold et al., 2011) has also been applied in SO studies on the conjunctive use issue (Cai et al., 2015), but SWAT conceptualizes the groundwater system as water tanks, and highly simplifies groundwater flow processes. In areas with strong and complicated SW–GW interactions (e.g., groundwater discharge into streams, riverbed leakage, groundwater exfiltration as springs, groundwater recharge by irrigation water, etc.), physically based, fully integrated SW–GW modeling is highly desired to appropriately account for the critical processes. Neverthless, the complex modeling has been rarely attempted within the SO framework.

Many integrated SW–GW models have been developed, such as Hydrogeosphere (Brunner and Simmons, 2012), MIKE-SHE (Graham and Refsgaard, 2001), ParFlow (Kollet and Maxwell, 2006), CATHY (Weill et al., 2011) and GSFLOW (Markstrom et al., 2008; Tian et al., 2015). These models can provide a comprehensive and coherent understanding on the basin-scale water cycle. However, incorporating such complex models in optimization remains as a great challenge, because both gradient-based and heuristic optimization algorithms would encounter difficulties in this case. In gradient-based algorithms, like linear programming (e.g., Singh and Panda, 2012), dynamic programming (Prasad et al., 2006), and fuzzy dynamic programming (e.g., Zeng et al., 2010), calculation of derivatives is a key step. The integrated models represent "black-box" functions whose derivatives cannot be analytically determined, while finite-difference approximation of the derivatives is laborious and may encounter the discontinuity problem. On the other hand, heuristic algorithms, such as genetic algorithm (GA) (Goldberg, 1989; Holland, 1975), particle swarm optimization (PSO) (Clerc and Kennedy, 2002) and shuffled complex evolution (SCE-UA) (Duan et al., 1992), require no derivative-calculation and are more promising for finding global optima. But they usually involve a very large number of iterations, and the optimization would be extremely time-consuming with complex models. A potential solution to this would be to employ surrogate modeling.

In general, surrogate modeling refers to replacing a complex model with much simpler and computationally cheaper mathematical relationships in an iterative model evaluation process (e.g., Monte Carlo Simulation, heuristic optimization, etc.). There are two major types of surrogate modeling approaches. One is response surface approaches aimed at finding a data-driven relationship between multiple explanatory variables and a model output variable. This type of approaches have been increasing used in optimization studies recently (Razavi et al., 2012). Representative ones include Probabilistic Collocation Method (PCM) (e.g., Zheng et al., 2011; Wu et al., 2014), Kriging (e.g., Baú and Mayer, 2006), Support Vector Machine (SVM) (e.g., Cai et al., 2015) and radial basis function (RBF) (e.g., Regis and Shoemaker, 2007). There are two typical strategies to perform a surrogate-based optimization using response surface. One is batch approaches (e.g., Johnson and Rogers, 2000; Liong et al., 2001; Cai et al., 2015) which establish globally satisfactory response surfaces once for all, using a very large training set. The other is adaptive approaches which use a small training set to establish initial response surfaces (usually unsatisfactory) and iteratively update them with additional training points (e.g., Forrester and Keane, 2009; Ostfeld and Salomons, 2005; Regis and Shoemaker, 2007). DYCORS (DYnamic COordinate search using Response Surface models) by Regis and Shoemaker (2013) is a typical adaptive response surface approach. The other type of surrogate modeling approaches is often referred to as model reduction or reduced-order modelling (Castelletti et al., 2012; McPhee and Yeh, 2008; Pasetto et al., 2011; Razavi et al., 2012), which yields a low-order, physically based, dynamic surrogate model of the original complex model. This type of approaches has also been adopted in optimization studies (e.g., Galelli et al., 2010). Although different surrogate modeling approaches have been employed for both surface water modeling (e.g., Ostfeld and Salomons, 2005; Cai et al., 2015) and groundwater modeling (e.g., Johnson and Rogers, 2000; Mugunthan and Shoemaker, 2006), they have been rarely used for fully integrated SW–GW modeling (Wu et al., 2015).

This study investigated the human-nature water conflicts in Heihe River Basin (HRB) in inland China. Farmlands in the middle HRB divert a great amount of the river flow, significantly reducing the water available to the lower HRB, a Gobi desert area with poor vegetation. Before 2000, the ecosystem in the lower HRB had experienced a fast degradation, and the end lake of the Heihe River were even dried out in certain years. A river flow regulation, starting from 2000, has refrained the surface water diversion, but stimulated groundwater pumping and caused a decline of the regional groundwater storage. The water issues in HRB are typical of inland river basins in the world. This study performed temporal optimization for the conjunctive use of river flow and groundwater in the Zhangye Basin (ZB), the core part of the middle HRB. GSFLOW and DYCORS were used as the integrated SW–GW model and surrogate-based optimization approach, respectively. The study objective was to explore how integrated hydrological modeling and surrogate-based optimization could benefit each other, and collaboratively solve complex real-world problems. The study results can also provide insights into the water resources management in HRB.

2. Data and method

2.1. The DYCORS algorithm

This study chose DYCORS (Regis and Shoemaker, 2009, 2013) as the surrogate-based optimization approach. The surrogate modeling in DYCORS adopts radial basis functions (RBFs) as the response surfaces. It has been demonstrated that, for optimization problems involving a complex hydrological model, DYCORS can effectively find optimal (or near-optimal) solution(s) with a reasonable computational cost (Espinet et al., 2013; Li et al., 2015). The main reason for using DYCORS in this study was two-fold. First, DYCORS adaptively updates its response surfaces during the optimization process. This is an innovative design which would substantially enhance the algorithm's searching efficiency. Second, the response surface approach in DYCORS aims to emulate a specific aspect(s) of the original model through a data training procedure, rather than to replace the original model as a whole based on a model-reduction analysis. This would offer great flexibility to the adaptive searching in DYCORS.

Let $y = f(\boldsymbol{x})$ denote a computationally expensive function, which incorporates a complex "black-box" model, to be minimized, where x represents a vector of decision variables. Also, let $g(\boldsymbol{x})$ denote a surrogate model for $f(\boldsymbol{x})$. In general, DYCORS takes the following steps:

i) Randomly sample n_0 initial points of $\boldsymbol{x}_i$ ($i = 1, 2, \ldots, n_0$) and compute the corresponding objective value y_i. Let $\mathcal{A}$ denote the set of the sampled points, and $\mathcal{B}$ denotes the corresponding set of objective function values. In this initial step, we have the iteration number (denoted as I) equal to 1, $\mathcal{A} = \{\boldsymbol{x}_1, \ldots \boldsymbol{x}_{n_0}\}$, and $\mathcal{B} = \{y_1, \ldots y_{n_0}\}$, and the cumulative number of objective function evaluations (denoted as N) equals to n_0. In the following steps, $\mathcal{A}$

Please cite this article in press as: Wu, X., et al., Optimizing conjunctive use of surface water and groundwater for irrigation to address human-nature water conflicts: A surrogate modeling approach. Agric. Water Manage. (2015), http://dx.doi.org/10.1016/j.agwat.2015.08.022

and $\mathcal{B}$ are expanded as more points are sampled, and N increases accordingly.

ii) Build the surrogate model g_I based on $\mathcal{A}$ and $\mathcal{B}$, using RBF. RBF is an interpolation-based response surface method, whose details can be found elsewhere (Powell, 1992).

iii) Generate k new points $\boldsymbol{x}_1,\ldots\boldsymbol{x}_k$ by perturbing the current points in $\mathcal{A}$. k is a small number, much less than n_0. This perturbation step is critical to the efficiency and effectiveness of DYCORS. Details about this step can be found in (Regis and Shoemaker, 2013). In brief, in the high-dimensional space of $\boldsymbol{x}$, each dimension is first assigned a probability of being perturbed based on certain rules (Tolson and Shoemaker, 2007). The dimensions to perturb in the current step are then randomly picked. On those picked dimensions, each point in $\mathcal{A}$ receives Gaussian perturbations. Each of the mutated points gets a score based on its distance to the original points in $\mathcal{A}$, as well as its objective function value approximated by g_I (denoted as $\hat{y}$). A point with a larger distance and smaller $\hat{y}$ value achieves a higher score. The k points with the highest scores are selected as the candidates.

iv) Compute the objective function values $y_1,y_2,\ldots,y_k$ for $\boldsymbol{x}_1$, $\boldsymbol{x}_2,\ldots,\boldsymbol{x}_k$, using the original objective function $y=f(\boldsymbol{x})$. Let $I=I+1$, $\mathcal{A}=\mathcal{A}\cup\{\boldsymbol{x}_1,\ldots\boldsymbol{x}_k\}$, $\mathcal{B}=\mathcal{B}\cup\{y_1,\ldots y_k\}$, and $N=N+k$.

v) Check the termination criterion. If N reaches a pre-determined number $N_{\max}$, identify the best point in $\mathcal{B}$ and its corresponding decision variable vector is selected as the final solution x^*. Otherwise, go back to Step ii for the next iteration. It is worth pointing out that the original DYCORS algorithm does not check the convergence. Its rationale is to keep the search going on within an allowed computing timeframe. A recent study (Wu et al., 2015) investigated how to check the convergence in adaptive surrogate-based optimization. Nevertheless, our study still used the original termination criterion of DYCORS.

DYCORS typically requires several hundreds of evaluations of the original model, which represents a high computing efficiency. But the computation is still laborious when a basin-scale integrated SW–GW model is involved in the objective function. To further reduce the computational cost, this study adopted a "reuse" strategy, as explained below. Conceptualize the objective function as $y=f\left(\boldsymbol{H}\left(\boldsymbol{x},\boldsymbol{\theta}\right),\boldsymbol{\phi}\right)$, where H represents hydrological variables simulated by the integrated model, which are dependent on the decision variable vector $\boldsymbol{x}$ and the hydrological model's parameters θ; and $\boldsymbol{\Phi}$ denotes all the parameters in the objective function, except $\boldsymbol{\theta}$. In each optimization, DYCORS generates $N_{\max}$ realizations of $\boldsymbol{x}$ and achieves the respective H ($\boldsymbol{x},\boldsymbol{\theta}$) using the original model. If all the parameters and inputs of the hydrological model keep the same across different optimization scenarios, the realizations of x and H ($\boldsymbol{x},\boldsymbol{\theta}$) obtained in one scenario can be retained and reused to derive the initial sets of $\mathcal{A}$ and $\mathcal{B}$ for the other scenarios. The benefit of the reuse in the other scenarios is two-fold. First, evaluations of the original complex model are no longer needed in Step i. Second, because DYCORS now starts with $\mathcal{A}$ and $\mathcal{B}$ of a larger size, the initial surrogate models could be more reliable, and therefore the terminal criterion $N_{\max}$ could be reduced. In this study, the initial sample size n_0, number of new points in each iteration k and terminal criterion $N_{\max}$ were set to 10, 2 and 400, respectively. All other parameters of DYCORS were default.

2.2. Study area

The Heihe River Basin (HRB) is the second largest inland river basin in China (Fig. 1), with a total area of about 130,000 km^2. Its landscape, climate, ecosystem and societal system are typical of China's inland river basins. The Heihe River originates from Qilian Mountains and ends in the East Juyan Lake (i.e., the river's terminal lake) in Inner Mongolia, and its mainstream has a length of about 820 km. Yingluoxia and Zhengyixia are the two points which divide the mainstream into upper, middle and lower parts (Fig. 1b). The upper HRB in Qilian Mountains provides a large amount of surface runoff (over 3.5 billion m^3/year) to the middle HRB where farmlands in oases consume a large share of the runoff and significant amount of groundwater. The lower HRB, the Gobi desert area, has a fragile ecosystem highly depending on the surface water from the middle HRB.

Due to the rapidly increased irrigation water consumption in the middle HRB, the streamflow through Zhengyixia experienced a significant decrease in the 1990s, leading to serious ecological problems (e.g., drying-up of the terminal lakes and dying of culturally significant *Populus euphratica* trees) in the lower HRB (Chen et al., 2005; Niu et al., 2011; Wang et al., 2015). The situation had not been alleviated until a water allocation plan was officially implemented by the central government in 2000. The plan requires bottom-line outflows at Zhengyixia under different inflow conditions at Yingluoxia (Liu et al., 2010; Liu and Wang, 2012). The plan actually specifies five inflow conditions and the respective outflow requirements, and a "water allocation curve"(WAC) can be derived based on the discrete points, as illustrated by Fig. 2. WAC aims to secure the environmental flow for restoring the downstream ecosystem, and essentially represents a rule of water allocation between the local economy and the natural ecosystem. Although the water diversion in the middle HRB has been refrained by the regulation and the recovery of the ecosystem has been observed, the WAC was not met in most of the years in 2000–2008 (Fig. 2). The gap was even larger in those wetter years (i.e., 2003, 2007 and 2008). Moreover, in recent years, irrigation districts in the middle HRB began to rely more and more on groundwater to irrigate. The increasing groundwater pumping has been largely unregulated, which has caused a fast decline of groundwater head (about 0.1–1 m per year, according to well observations) and posed potential environmental and ecological risks to the middle HRB (Ji et al., 2005, 2006).

This study was focused on the Zhangye Basin (ZB), a core part of the middle HRB which contains the majority of the irrigation districts in HRB. The hydrological modeling domain (Fig. 1b) is bounded by Qilian Mountains on the south, the Bei Mountains on the north, the Jiuquan-west Basin on the west and the Maying Basin on the east. Farmlands account for 31.4% of the domain, and the left area is composed of deserts (53.2%), and grasslands (12.8%). The annual precipitation is 190 mm on average, but the annual potential evapotranspiration (ET) ranges from 1200 to 2200 mm, indicating a highly water-limited environment. The surface water boundary inflow is about 2.32 billion m^3 per year in total, 74% of which is through Yingluoxia. Agriculture is the major activity in ZB, and the main crops are corn and winter-wheat. There are 20 irrigation districts within the domain (Fig. 1b). Based on the data collected from the water resources authority of the Zhangye City, in 2000–2008, the irrigation water consumed by the farmlands in this area was 1.25 billion m^3 per year on average, 71% from the main Heihe River and the left from the local aquifer. Water diverted from the main stream is conveyed and distributed by a complex aqueduct system, often over a long distance. Groundwater pumped from wells is usually fed into adjacent fields.

2.3. The GSFLOW model

A previous study (Wu et al., 2014) has established an integrated SW–GW model for the Zhangye Basin (ZB) using GSFLOW, and this optimization study was based on the same model. GSFLOW (Markstrom et al., 2008) is a modeling platform developed by USGS, which couples the surface hydrology model PRMS (Leavesley et al., 1983) with MODFLOW. It performs 2-D surface hydrology simulation and 3-D groundwater simulation. Hydrologic response units

Please cite this article in press as: Wu, X., et al., Optimizing conjunctive use of surface water and groundwater for irrigation to address human-nature water conflicts: A surrogate modeling approach. Agric. Water Manage. (2015), http://dx.doi.org/10.1016/j.agwat.2015.08.022

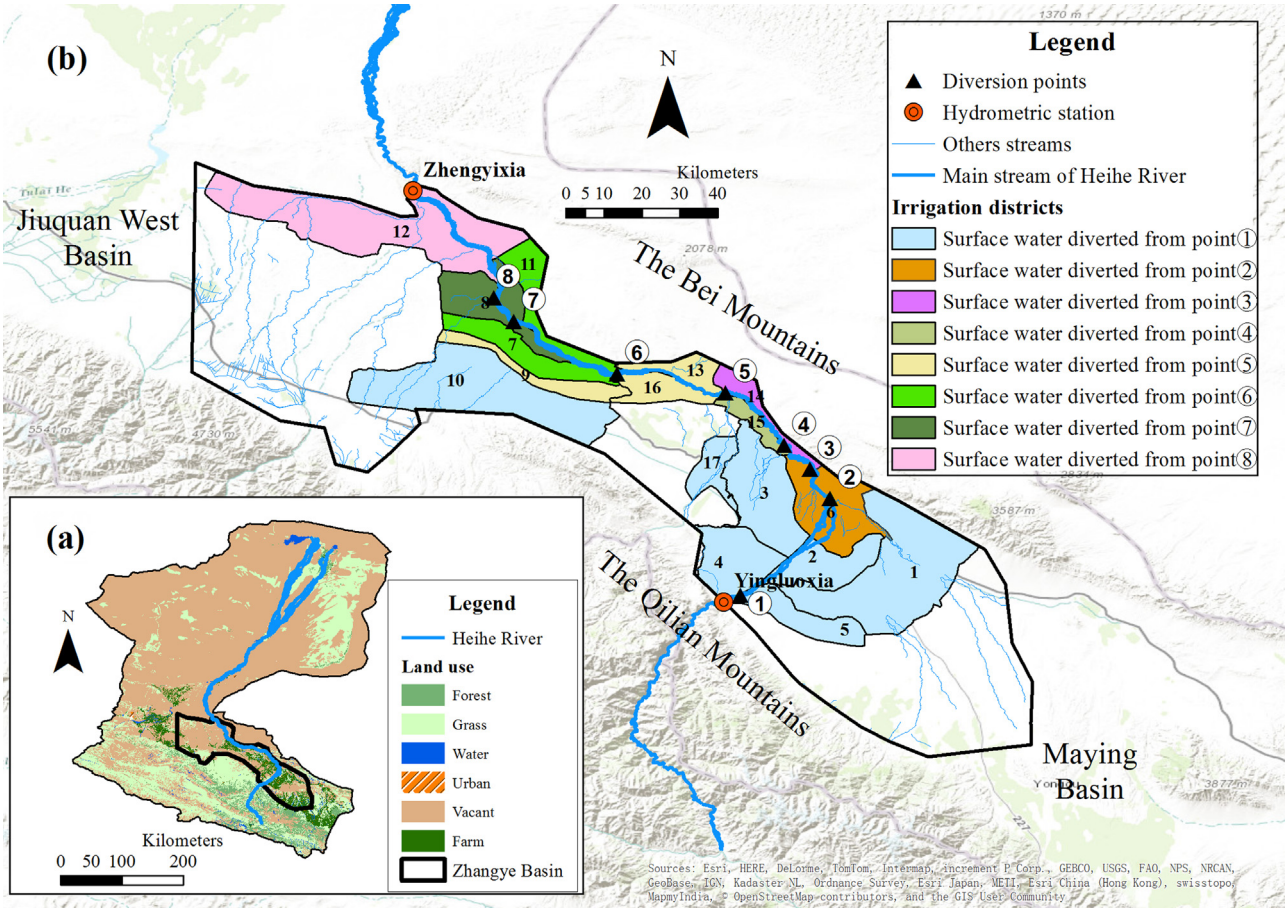

Fig. 1. Study area. (a) Heihe River Basin; and (b) the modeling domain (Zhangye Basin).

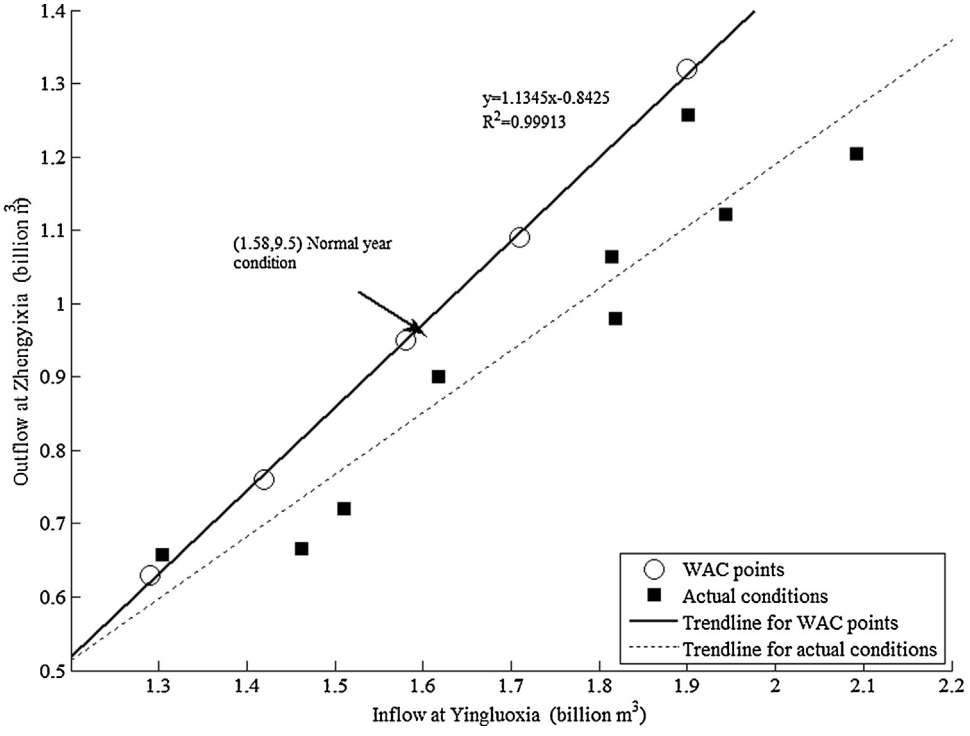

Fig. 2. The water allocation curve (WAC) and actual inflow-outflow conditions of the modeling domain.

Please cite this article in press as: Wu, X., et al., Optimizing conjunctive use of surface water and groundwater for irrigation to address human-nature water conflicts: A surrogate modeling approach. Agric. Water Manage. (2015), http://dx.doi.org/10.1016/j.agwat.2015.08.022

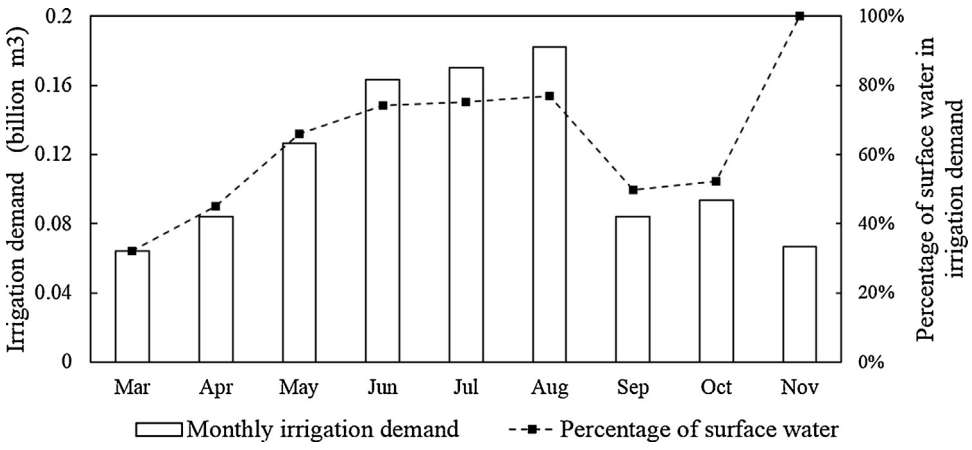

Fig. 3. Monthly irrigation water demands of the 17 irrigation districts

(HRUs), either regular grids or irregular polygons, are the basic computing units of the surface domain. The subsurface domain is discretized into finite difference girds. GSFLOW defines "gravity reservoir" as a storage in which an HRU exchanges water with the MODFLOW grid(s) it intersects. In GSFLOW, between the soil zone and aquifer, a vadose zone is defined and handled by the Unsaturated Zone Flow package (UZF1) (Richard et al., 2006). Streams and lakes are simulated using the Streamflow Routing package (SFR2) (Richard and David, 2010) and Lake package (LAK3) (Michael and Leonard, 2000), respectively. Stream-aquifer exchanges are calculated using Darcy's law, based on the head difference between a reach and the subsurface grid(s) it intersects. More details about GSFLOW and its components can be found in Markstrom et al. (2008).

The current version of GSFLOW can handle dynamic inflow into a stream segment, but flow withdrawn from the segment must be constant within a stress period. Thus, GSFLOW is unable to flexibly handle time-variant flow diversion data. Wu et al. (2014) proposed an alternative way to account for daily flow diversion in GSFLOW, which was adopted by this study. In the alternative way, a tiny stream segment is first separated out at the diversion point. For this "dummy" segment, daily inflow rates and a constant flow withdrawn rate are then both specified, ensuring that the difference between the withdrawn and inflow is equal to the actual diversion rate on each simulation day. Of the 20 irrigation districts in the modeling domain, 17 (labeled in Fig. 1b) use water from the main river, and the others use water from tributaries. The 17 districts draw water from over 50 diversion points between Yingluoxia and Zhengyixia. To simplify the simulation-optimization, adjacent diversion points were combined and the actual points were conceptualized into 8 virtual ones in the model. In Wu et al. (2014), the stress period for groundwater pumping was set to one year, and therefore within a year the pumping rate (in billion m^3 per unit time) of each district is constant in time. To perform temporal optimization, this study reduced the stress period length to one month. Spatially, the pumping rate varies across districts. Within each district, all grids associated with farmland HRUs are assumed to have a same pumping rate in one stress period.

2.4. Water use strategy

The districts use surface water and groundwater conjunctively to meet their irrigation needs. The decision process of water use can be conceptualized as follows. In the *i*th time period, the *j*th district first decides the total amount of water required by its farmlands, denoted as F_{ij}. F_{ij} depends on many factors including crop types, growing season, cultivating area, irrigation methods, water-saving measures, etc. On the other hand, following the water regulation, each district is allowed to have a maximal amount of water diversion, denoted as d_{ij}. Due to evaporation and seepage losses of the aqueduct system, the surface water that eventually reaches the fields would be $\eta_j \cdot d_{ij}$, where η_j represents an efficiency coefficient, assumed to be time-invariant in this study. Then, the district would pump groundwater of an amount p_{ij} which equals to $F_{ij} - \eta_j \cdot d_{ij}$. Such conceptualization reflects the fact that in ZB the groundwater exploitation has not been well regulated, and therefore the regulation on flow diversion has led to more pumping.

In this study, the values of η_j were determined based on reports provided by the local water resources authority of the Zhangye City, ranging from 0.48 to 0.57 in different irrigation districts, and the values of F_{ij} were estimated as $d_{ij}^0 \cdot \eta_j + p_{ij}^0$, where d_{ij}^0 and p_{ij}^0 are the monthly diversion amounts and pumping rates according to the historical data we collected, respectively. This is equivalent to assuming that the irrigation demands were well satisfied historically (i.e., the demands were equal to the respective actual supplies), and no water-saving strategies are to be implemented (i.e., η_j does not change over time). Historical data of d_{ij}^0 and p_{ij}^0 were collected from the local water resources authority as well, and re-scaled to the monthly resolution. The estimated historical monthly demands of the 17 districts, averaged over 2000–2008, are illustrated in Fig. 3. The monthly percentages of surface water in the total irrigation demand (denoted as r_i) are also plotted in the figure. r_i is equal to $\sum_j d_{ij}\eta_j / \sum_j F_{ij}$. As indicated by Fig. 3, the growing season in ZB extends from April to October, and May to August is the main irrigation period. The irrigation in March and November is mainly for maintaining proper soil moisture, heat and salinity before the growing season. Fig. 3 also shows that in the main irrigation season (i.e., May to August), the irrigation mostly consumes surface water. In November, the irrigation exclusively uses surface water.

2.5. Formulation of optimization problem

The optimization problem investigated in this study is to maximize the annual storage change of saturated zone, denoted as ΔS (in billion m^3), under a given outflow constraint Q_0 at Zhengyixia, which emulates the current water regulation regime. The value of Q_0 can be arbitrarily set, and different values represent different management scenarios. ΔS is a positive value when the storage increases, and a negative value when the storage decreases. Thus, a more positive ΔS value indicates a better-off situation (i.e., increase of the groundwater storage in ZB). The decision variables, $\mathbf{X} = (X_1, X_2, \ldots X_{12})$, are monthly total volumes of surface water diverted

Table 1
Eight optimization scenarios examined in this study.

Type of Q_0 constraint	Actual water Demand	10% demand reduction	20% demand reduction	30% demand reduction
No-flow-decrease	A1	A2	A3	A4
Water allocation curve	B1	B2	B3	B4

Table 2
Inflow conditions and outflow constraints of the optimization experiments (Unit: billion m^3).

Inflow condition		Q_0 constraint				
Year	Q_y	B1-B4	A1	A2	A3	A4
2000	1.463	0.819	0.666	0.743	0.827	0.908
2001	1.305	0.645	0.657	0.707	0.754	0.828
2002	1.618	0.992	0.900	0.983	1.081	1.153
2003	1.901	1.314	1.257	1.330	1.421	1.501
2004	1.510	0.871	0.720	0.771	0.858	0.938
2005	1.818	1.218	0.979	1.058	1.154	1.196
2006	1.814	1.211	1.064	1.161	1.217	1.285
2007	2.092	1.525	1.204	1.309	1.427	1.516
2008	1.944	1.353	1.122	1.174	1.262	1.329

from the main river (in billion m^3). The optimization problem can be mathematically expressed as

$$\begin{aligned} &\underset{\boldsymbol{X}}{Max}\,\Delta S(\boldsymbol{X}) \\ &s.t. \\ &Q_z \geq Q_0 \\ &\sum\nolimits_{j\in I_1} d_{ij} \leq Q_{il}, \forall i, l \end{aligned} \tag{1}$$

where Q_z is the annual outflow at Zhengyixia simulated by the GSFLOW model; Q_{il} represents the monthly streamflow at the lth (l = 1, 2,. . ., 8) diversion point (Fig. 1b) before the potential diversion takes place; I_l denotes the set of irrigation districts served by the lth diversion point (refer to Fig. 1b). All the flux variables are in billion m^3. The second constraint ensures that the potential diversion volume not exceed the available streamflow. Q_z and Q_{il} are output variables of the calibrated GSFLOW model. Because this study addressed a temporal optimization issue, rather than a spatial one, it was assumed that the amounts of diverted surface water change proportionally among all the districts. To ensure that X_i varies between 0 and its maximal value, that is, $\sum_j \left(F_{ij}/\eta_j\right)$, the following assumptions have been added: 1) given an increase of X_i (i.e., ΔX_i >0), the districts would enhance their water diversion in proportion to p_{ij}^0/η_j; and 2) given a decrease of X_i (i.e., ΔX_i <0), the districts would reduce their water diversion in proportion to d_{ij}. These two additional assumptions can be formulated as

$$d_{ij} = \begin{cases} d_{ij}^0 + \Delta X_i \dfrac{d_{ij}^0}{\sum_j d_{ij}^0}, & \Delta X_i < 0 \\ d_{ij}^0 + \Delta X_i \dfrac{p_{ij}^0/\eta_j}{\sum_j (p_{ij}^0/\eta_j)}, & \Delta X_i \geq 0 \end{cases} \tag{2}$$

The optimization problem in form of Eq. (1) can be further transformed into a no-constraint form by adding penalty items, which is a common strategy to perform searching-based optimization with constraints (Deb, 2000). In this study, two penalty items, $P(Q_z)$ and $P(Q_{il})$, were defined, as

$$P(Q_z) = \begin{cases} 0, & Q_z \geq Q_0 \\ \omega \cdot |Q_z - Q_0| & Q_z < Q_0 \end{cases} \tag{3}$$

$$P(Q_{il}) = \begin{cases} 0 & Q_{il} \geq \sum\limits_{j\in I_l} d_{ij} \\ \omega \cdot |Q_{il} - \sum\limits_{j\in I_l} d_{ij}|, & Q_{il} < \sum\limits_{j\in I_l} d_{ij} \end{cases} \tag{4}$$

where ω is a coefficient which was set to 5 based on preliminary trial-and-error tests. Hence, the optimization problem can be transferred into:

$$\underset{\boldsymbol{X}}{Min} y = -\Delta S(\boldsymbol{X}) + P(Q_z) + \sum\nolimits_{i=1}^{12} \sum\nolimits_{l=1}^{8} P(Q_{il}) \tag{5}$$

In the DYCORS procedure, given a candidate point of $\boldsymbol{X}$, ΔX_i is first calculated as $\left(X_i - \sum_j d_{ij}^0\right)$. Then, d_{ij} is determined based on Eq. (2), and the groundwater pumping rates p_{ij} is calculated as (F_{ij} - $\eta_j \cdot d_{ij}$). If the original integrated model is used to evaluate the objective function Eq. (5), the derived d_{ij} and p_{ij} are fed into the model to achieve Q_z, Q_{il} and ΔS. If the surrogate model (i.e., RBF in DYCORS) is used instead, the objective function approximation (i.e., $\hat{y}$) can be directly derived from d_{ij} and p_{ij}.

In this optimization problem, the irrigation demand F_{ij} and flow constraint Q_0 represent two key conditions. This study investigated 8 optimization scenarios based on four different levels of irrigation demand and two types of flow constraint, as summarized in Table 1. It is assumed that the reduction rates of irrigation demand are uniformly applied to each district in each month (i.e., to every F_{ij}). Scenarios A1 to A4 represent a no-flow-decrease situation, in which the Q_0 constraint adopts the outflows modeled at different levels of F_{ij} (Table 2). Scenarios B1 to B4 represent a regulation scheme in which the WAC must be met, and for these scenarios, the Q_0 constraint does not vary with the level of F_{ij} (Table 2). As Table 2 indicates, 9 inflow conditions (i.e., observed annual flow rates at Yingluoxia, denoted as Q_y) were considered. Therefore, this study performed 72(=8 × 9) optimization experiments in total. In each experiment, the GSFLOW model was run for two consecutive years with duplicated model inputs and parameters. The first year is regarded as the "warm-up" period which helps avoid abrupt fluctuation of water stored in soil zone and unsaturated zone. All the optimization experiments were programmed using MATLAB.

Please cite this article in press as: Wu, X., et al., Optimizing conjunctive use of surface water and groundwater for irrigation to address human-nature water conflicts: A surrogate modeling approach. Agric. Water Manage. (2015), http://dx.doi.org/10.1016/j.agwat.2015.08.022

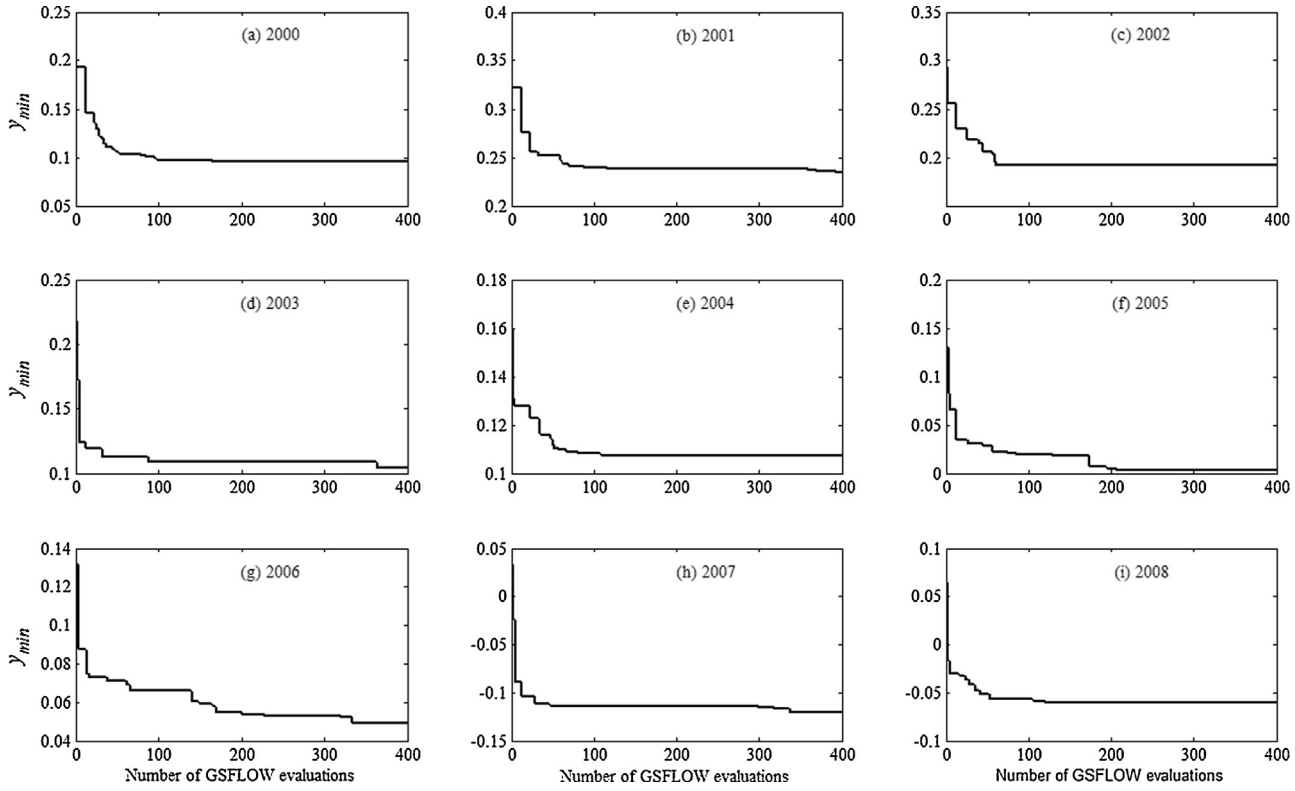

Fig. 4. Change of the minimal objective function value (y_{min}) during the DYCORS searches in Scenario A1. (a)–(i): nine inflow conditions of year 2000–2008.

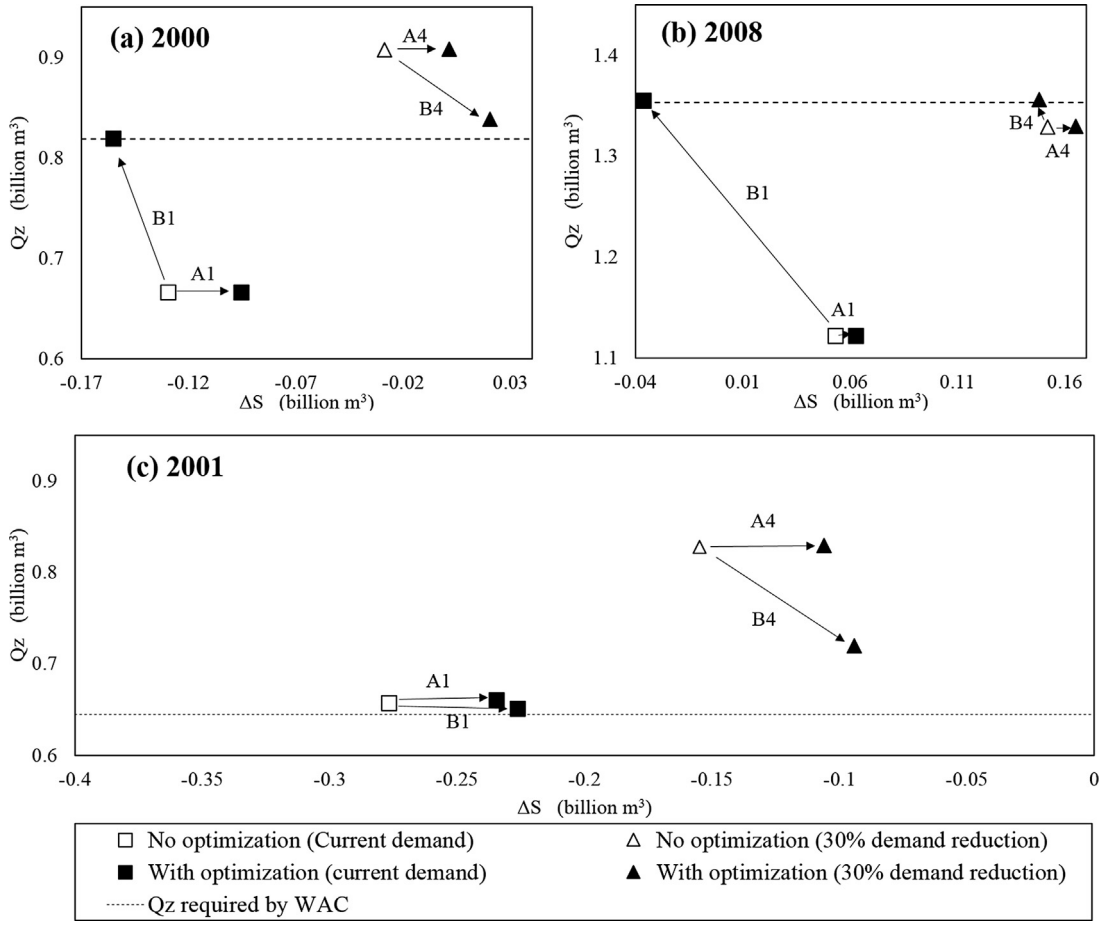

Fig. 5. Optimization results of selected experiments in Scenario A1, B1, A4 and B4. (a) inflow condition of year 2000; (b) inflow condition of year 2008; and (c) inflow condition of year 2001.

Please cite this article in press as: Wu, X., et al., Optimizing conjunctive use of surface water and groundwater for irrigation to address human-nature water conflicts: A surrogate modeling approach. Agric. Water Manage. (2015), http://dx.doi.org/10.1016/j.agwat.2015.08.022

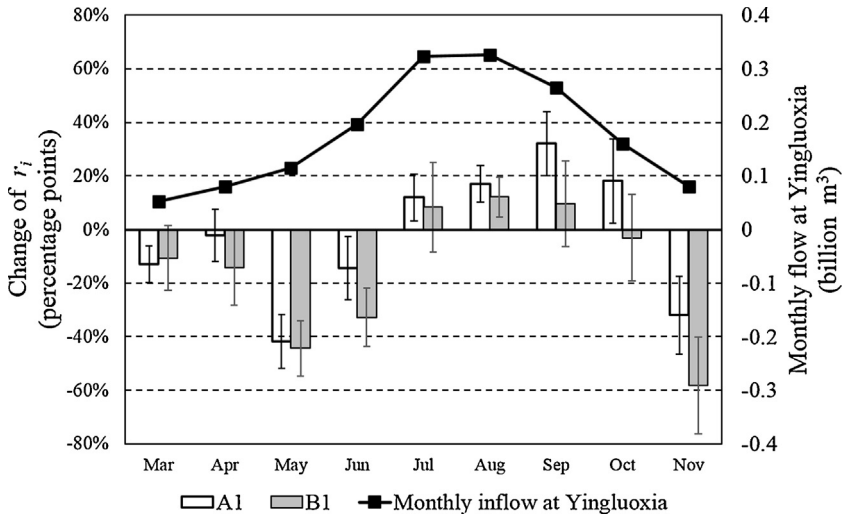

Fig. 6. Changes of the surface water percentages (r_i) before and after the optimization. The distance between two error bars represents one time the standard deviation. The left Y axis represents the changes of r_i, and the right Y axis represents the monthly inflow at Yingluoxia.

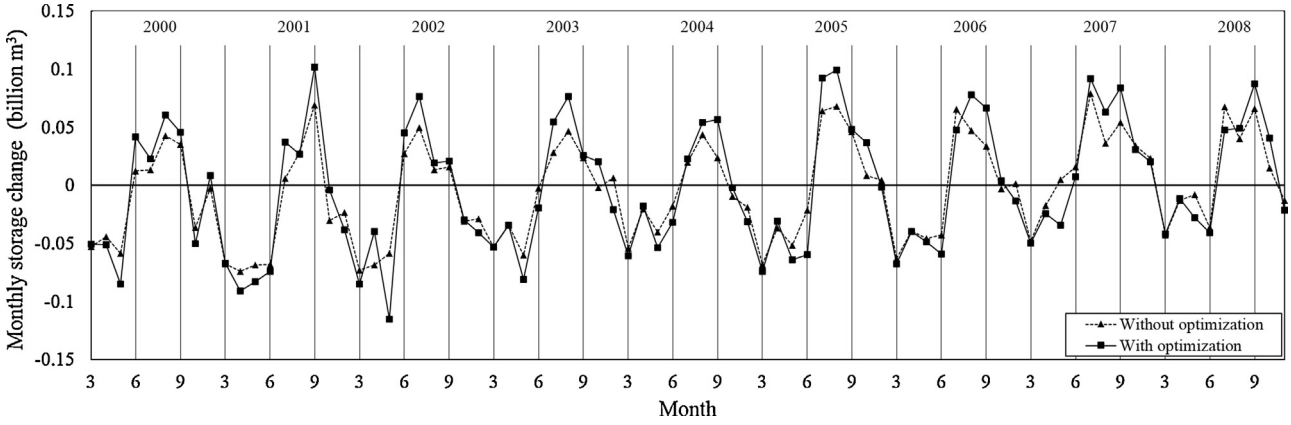

Fig. 7. Monthly groundwater storage changes with and without the optimization in Scenario A1. The *x* -axis presents the March-to-November periods of 2000–2008.

3. Results and discussion

3.1. Efficiency and effectiveness of DYCORS

Fig. 4 demonstrates the evolution of minimal objective function (i.e., Eq. (5)) value, denoted as y_{min}, during the DYCORS searches in Scenario A1. In all of the nine experiments, y_{min} decreased rapidly in the first 100 GSFLOW evaluations, and received no significant improvement after 200 evaluations. $N_{max} = 400$ is sufficient to stop the searches in this case. All other experiments had the similar convergence speed. In this study, a two-year GSFLOW evaluation takes about 8 min on a high-performance CPU core (4.4 GHz), and an optimization experiment with 400 GSFLOW evaluations takes about 2.5 days to finish. As discussed in Section 2.2, one experiment can use GSFLOW outputs from a previous one (with the same inflow condition) to establish its initial set of $\mathcal{B}$. It has been found that, with this "reuse" strategy, 150 GSFLOW evaluations are sufficient to terminate an optimization experiment in this study. Eventually, the 72 experiments were executed in parallel on 36CPU cores (4.4 GHz), and were finished in about 3.5 days. The "reuse" strategy helped reduce about 30% of the computational cost. Considering the model complexity and the large number of optimization experiments, the computation by DYCORS was very efficient.

Fig. 5 illustrates optimization results of the 12 experiments in Scenarios A1, B1, A4 and B4 with the inflow conditions of years 2000, 2001 and 2008. Years 2000 and 2001 had very low inflow rates (1.46 and 1.31 billion m^3, respectively), and 2001 is the only year that the WAC regulation was actually met. On the contrary, year 2008 had a high inflow rate of 1.94 billion m^3. Overall, Fig. 5 demonstrates the effectiveness of DYCORS, since significant changes of both Q_Z and ΔS have been resulted from the optimization. In the no-flow-decrease scenarios (A1 and A4), the improvement of ΔS (along the *x* axis) is significant for the two dry years (Figs. 5a and c), but minor for the wet year (Fig. 5b). This is because, under the wet condition of 2008, the local aquifer was sufficiently replenished already and the space for further improvement would be limited.

In Scenarios B1 and B4, when the WAC regulation is not met originally (Figs. 5a and b), the optimization suggests an upper-left movement, which means the increase of environmental flow is partially offset by the decline of groundwater storage. On the contrary, when the regulation is already met (Figs. 5a and c), the suggested direction of movement is lower-right, that is, to divert more and pump less. Given the conditions of years 2000 and 2001, Q_z is still above the WAC value even when the pumping approaches zero. Although mathematically appropriately, such optimization results are not useful for the water resources management, because the constraints are not realistic. The optimization results actually represent water wasting instead of water saving, as will be further demonstrated in Section 3.3.

Please cite this article in press as: Wu, X., et al., Optimizing conjunctive use of surface water and groundwater for irrigation to address human-nature water conflicts: A surrogate modeling approach. Agric. Water Manage. (2015), http://dx.doi.org/10.1016/j.agwat.2015.08.022

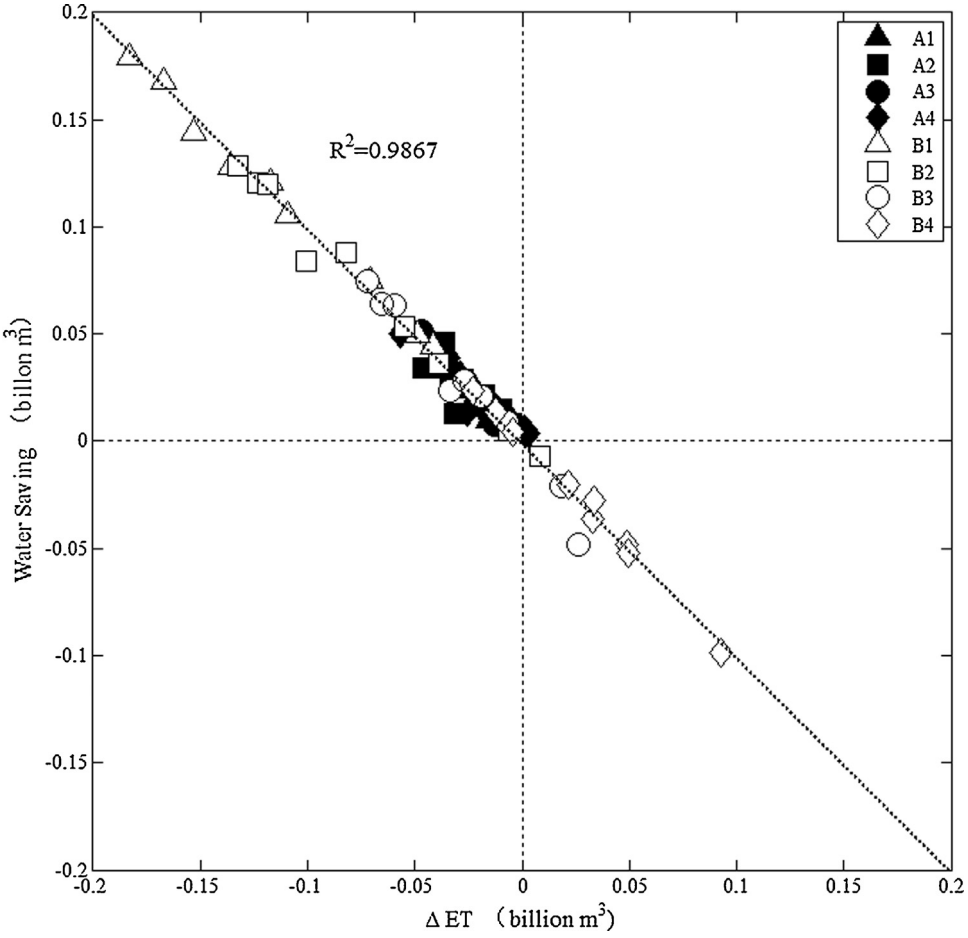

Fig. 8. Basin-wide water saving and change of ET at the 72 optimal solutions.

Table 3
Multiple regression models based on different scenarios.

Model	Scenarios	Sample size	β_0	β_1	β_2	β_3	Adjusted R^2
1	No optimization	36	−0.2574	−0.8112	0.9928	−0.7188	0.9490
2	Optimization	72	−0.2840	−0.6312	0.8270	−0.5542	0.9030

3.2. Optimized monthly diversion schedule

Fig. 6 shows the changes of r_i (i.e., the monthly percentage of surface water in total irrigation demand) achieved in Scenarios A1 and B1. The means and standard deviations of the nine different inflow conditions are presented in the figure. As indicated, the two scenarios exhibit a similar pattern of change. The patterns in all other six scenarios (not illustrated here) are also similar. In general, the optimization suggests a reduction of r_i in March to June and November, and an increase in July–October. Fig. 7 further compares the monthly groundwater storage changes with and without the optimization in Scenario A1. Although inter-annual variation presents, in general the optimization leads to a larger storage decline in May and June, and a more prominent storage recovery during July–September (i.e., the flood season). Figs. 6 and 7 together imply that the local aquifer actually serves as a huge "reservoir", and the optimization suggests releasing the "reservoir" storage before the flood season to create a sufficient storage capacity for the potential recharge during the flood season.

Heihe River Bureau, a trans-jurisdictional watershed management agency, has been empowered to regulate the diversion practices in ZB. In each year, the Bureau mandates certain time periods in which the diversion along the middle Heihe River is completely forbidden. Historically, the diversion-forbidden periods varied in different years, but were mainly in July–October, simply because the river flow was most abundant in these months (Fig. 6). Since 2004, the diversion practices were also prohibited on certain days in April and May. The rationale behind it is that April–May is a critical period for the vegetation growth in the lower HRB, and therefore the downstream desires more environmental flow in this particular period. Overall, the current diversion regulation considers only surface hydrology, with no attention paid to the groundwater system. Interestingly, as demonstrated by Fig. 6, the timing of diversion regulation suggested by the optimization is opposite to the present schedule, except for April. The important implication here is that, in river basins where groundwater plays an important role in the hydrological cycle, water resources management must fully account for SW–GW interactions; otherwise, inappropriate management decisions could be made.

3.3. Basin-scale water saving

From a basin-wide perspective, an increase of $(Q_Z + \Delta S)$ indicates an overall water saving in ZB, since Q_Z represents the surface

Please cite this article in press as: Wu, X., et al., Optimizing conjunctive use of surface water and groundwater for irrigation to address human-nature water conflicts: A surrogate modeling approach. Agric. Water Manage. (2015), http://dx.doi.org/10.1016/j.agwat.2015.08.022

water resource transferred from ZB to the lower HRB, while ΔS represents the variation of groundwater resource in ZB. Fig. 8 plots the change of $(Q_z + \Delta S)$ against the change of basin-wide ET, considering the optimal solutions of all the 72 experiments. $(Q_z + \Delta S)$ and ΔET show a nearly perfect 1:1 relationship ($R^2 = 0.9867$), which manifests that the basin-scale water saving suggested by the optimization is almost exclusively due to the reduction of ET. The small deviation of the points from the dashed trend line reflects the minor storage changes of soil, vadose zone, river channel, etc. For Scenarios A1 to A4, the total water saving ranges from 0.01 to 0.05 billion m^3, and predominantly turns into a positive change of ΔS (i.e., less storage decline or more storage recovery). On the contrary, for Scenarios B1 to B4 with the stringent WAC constraint, the saving shows a much larger variation, and is even negative in certain cases. The positive water saving is exclusively transformed to an increase of Q_z, and meanwhile the change of ΔS is negative. The negative saving occurs in situations when the WAC constraint is already met or can be met by reducing the irrigation demand without optimization. The above findings are consistent with the results in Fig. 5.

To further reveal the mechanism of water saving, the annual water budgets before and after the optimization in Scenario A1 were graphed in Fig. 9a. It clearly shows that, at an annual time scale, the optimization suggests less flow diversion and more groundwater pumping, resulting in a significant increase of stream leakage to aquifer, as well as a mild decrease of groundwater discharge to stream. Meanwhile, the decrease of flow diversion reduces the aqueduct seepage and therefore lowers the soil moisture content, which eventually reduces the ET from the aqueduct system and soil zone. Surface runoff and interflow are also reduced, because the soil moisture content is lowered. The overall effect is two-fold: the basin-wide ET is reduced and the regional groundwater storage is recovered. In Scenario A1, the change of ET (−0.025) is equivalent to the change of saturated zone storage (Fig. 9a). Similarly, Fig. 9b illustrates the water budget in Scenario B1. The changing pattern is similar. But the stringent WAC constraints conserve much more stream outflow and greatly stimulate the pumping. As a result, the stream leakage is further enhanced, but the groundwater storage change is negative in this case. Overall, Fig. 9 quantitatively demonstrates a typical depletion-and-capture process which has been long discussed (Theis, 1940; Konikow and Leake, 2014). Essentially, to meet the outflow constraints, the streamflow has to be "re-routed" by pumping via an underground "aqueduct".

3.4. Supporting the regional water management

The water management based on the WAC has been effective in providing more water to the lower HRB, and a recovery of the downstream ecosystem has been witnessed in recent years. However, if the districts in ZB do not refrain their irrigation water demand, the recovery will have to be at the cost of groundwater storage decline in the middle HRB (Tian et al., 2015). The potential decline would pose a significant risk to the ecosystem and sustainable development of ZB. To wisely manage the precious water resources from a basin-wide perspective, it is crucial to understand the interrelationship among the regional climate conditions (reflected by the inflow Q_y), human water needs (represented by the total irrigation water demand, denoted as D and equal to $\sum_{i,j} F_{ij}$), ecological water demand (satisfied by the outflow Q_z) and the groundwater storage (whose annual change is ΔS) in ZB. The integrated hydrological modeling and the surrogate-based optimization approach provide a unique opportunity to explore the interrelationship. Multiple linear regression was performed for the concerned variables, as follows:

$$\Delta S = \beta_0 + \beta_1 \cdot D + \beta_2 \cdot Q_y + \beta_3 \cdot Q_z + \epsilon \quad (6)$$

where ΔS is the annual storage change of saturated zone; D is the total irrigation water demand; Q_y is the annual inflow from Yingluoxia; Q_z is the annual discharge at Zhengyixia; all the β's are regression coefficients; and ϵ is a Gaussian error term. Two regression models for different optimization scenarios were built, one is for no-optimization scenarios and the other is for scenarios with the temporal optimization (Table 3). Model 1 considers the four demand (D) levels and nine inflow (Q_y) conditions and therefore used 36 samples. In Model 1, ΔS and Q_z were both simulated by the calibrated GSFLOW model. Model 2 considers the four levels of D, nine Q_y conditions and two types of Q_z constraint, and therefore used 72 samples. In model 2, only ΔS is the output of the GSFLOW model.

The regression coefficients of the two models were presented in Table 3. The high values of adjusted R^2 confirm the prominent interrelationship among the four variables. With the models, interpolation and/or extrapolation for other scenarios than the 108 (=36 + 72) sample scenarios can be easily performed, without additional optimization calculation. Thus, the models can provide an efficient support to water management decisions, such as determining how to adjust the irrigation demand. For example, assuming $\Delta S = 0$ (i.e., no storage decline allowed in ZB), $Q_y = 1.71$ (i.e., the average inflow condition) and $Q_z = 0.952$ (i.e., the average historical outflow rate), Model 1 predicts that the irrigation demand should be cut off by 10.2% without the temporal optimization. If the optimization is considered, Model 2 predicts a smaller reduction rate of 7.9%.

Appropriateness of the WAC regulation has been disputed for a long time, which reflects the water use conflict between the population of the midstream and the ecosystem of the downstream. The regression models can provide insights into the conflict. Fig. 10 illustrates optimized relationships between Q_z and Q_y for different ΔS values (different lines in the subplots) and irrigation demands (different subplots), as predicted by the regression Model 2. With the actual irrigation demand (Fig. 10a), the WAC points sit mostly between the lines of $\Delta S = -0.1$ and $\Delta S = -0.2$, close to the line of $\Delta S = 0.1$ in wet years and to the line of −0.2 in dry years. It indicates that, if both the irrigation demand and WAC keep unchanged, the storage decline in ZB is unstoppable. Even with the temporal optimization of surface water diversion, the decline would continue at a pace of −0.1–−0.2 billion m^3 per year, roughly the current pace of decline. Fig. 10b plots the relationship assuming a 20% reduction of irrigation demand. In this case, the WAC points are mostly adjacent to the line of $\Delta S = 0$, and close to the line of $\Delta S = -0.1$ only under extremely dry conditions. It suggests that, to maintain the groundwater storage in ZB while meeting the WAC regulation, at least a 20% reduction of irrigation demand in this region should be considered. Overall, Fig. 10 reveals that the WAC regulation has essentially transformed the human-nature conflict between the middle HRB and the lower HRB into the one inside the middle HRB. This is not a sustainable state, and a better solution to the existing human-nature conflicts is imperatively needed for HRB.

4. Conclusions

This study represents an early effort to link physically-based integrated surface water-groundwater (SW–GW) modeling with water management optimization via surrogate modeling. It clearly demonstrated how the integrated hydrological modeling and surrogate-based optimization could benefit each other, and collaboratively solve complex real-world management problems. To

Please cite this article in press as: Wu, X., et al., Optimizing conjunctive use of surface water and groundwater for irrigation to address human-nature water conflicts: A surrogate modeling approach. Agric. Water Manage. (2015), http://dx.doi.org/10.1016/j.agwat.2015.08.022

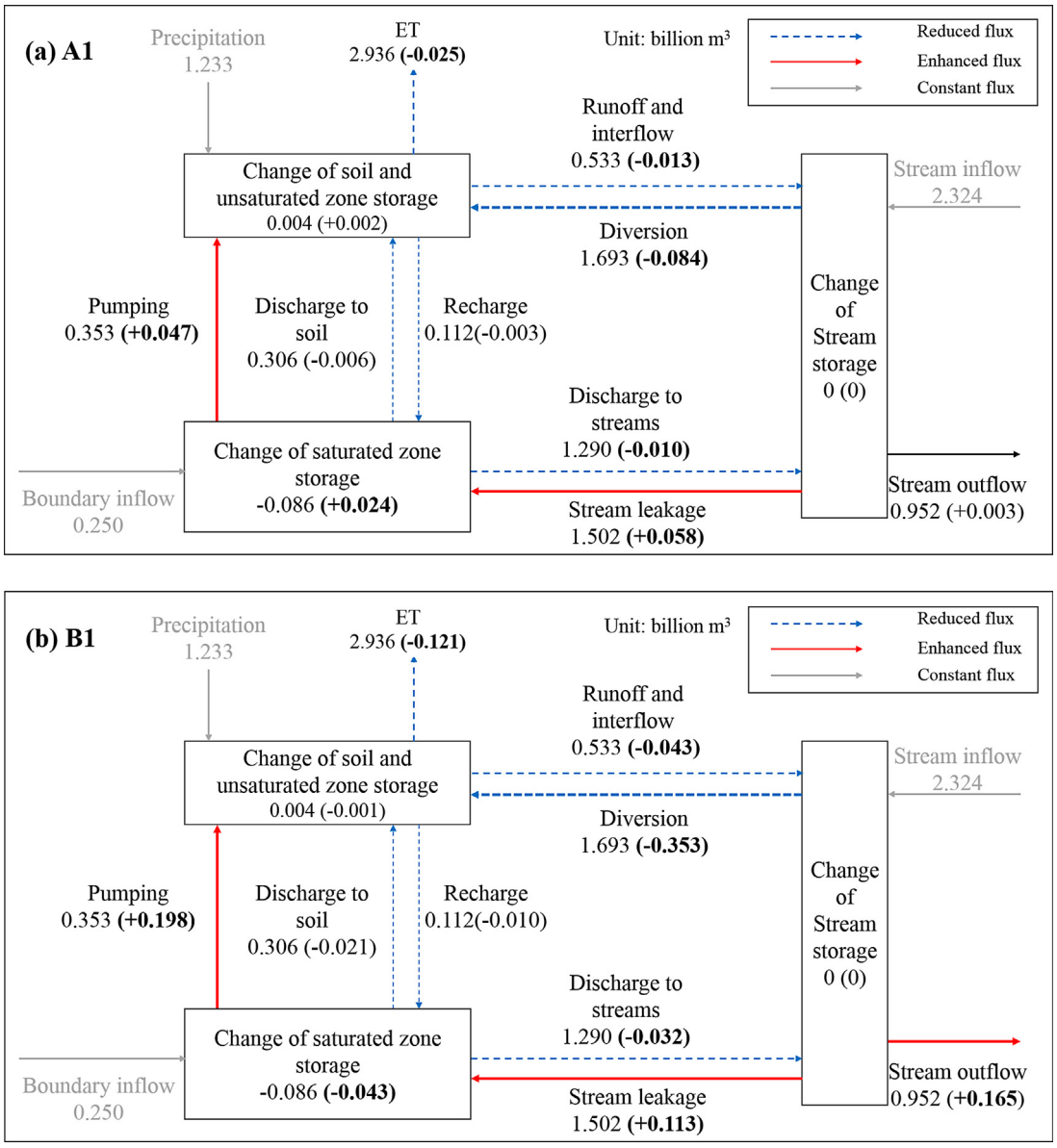

Fig. 9. Annual water budgets (averaged over 2000–2008) of the study area and changes of the budget (indicated by the numbers in parentheses) due to the optimization. (a) Scenario A1; and (b) Scenario B1.

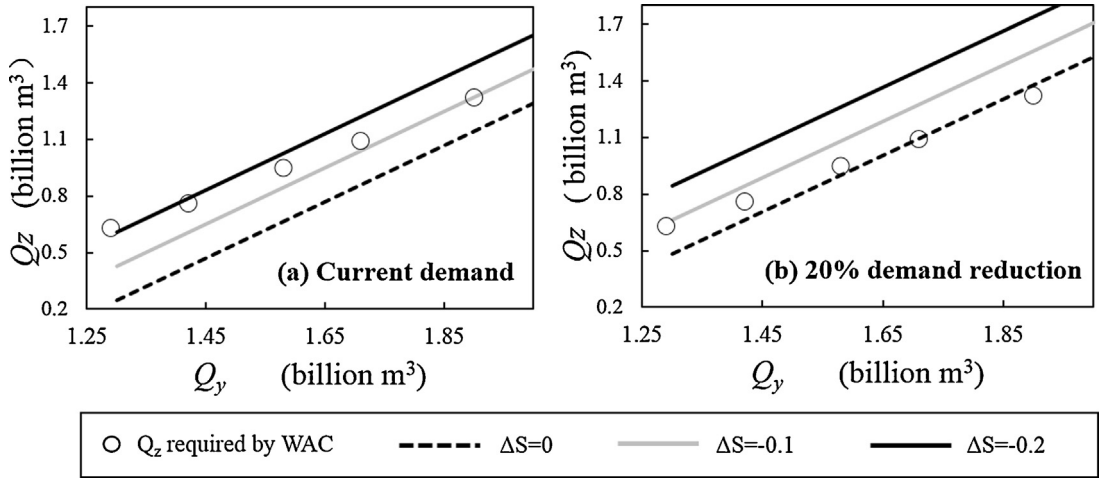

Fig. 10. Optimized relationships between the outflow Q_z and the inflow Q_y predicted by the regression Model 2. (a) considering the actual irrigation demand; and (b) considering a 20% demand reduction.

Please cite this article in press as: Wu, X., et al., Optimizing conjunctive use of surface water and groundwater for irrigation to address human-nature water conflicts: A surrogate modeling approach. Agric. Water Manage. (2015), http://dx.doi.org/10.1016/j.agwat.2015.08.022

address the significant water use conflicts (between human and nature, as well as between upstream and downstream) in the Heihe River Basin (HRB), which are typical water problems in inland river basins, a temporal optimization on the conjunctive use of surface water and groundwater for irrigation was performed. The major study findings include the following. First of all, with the surrogate modeling approach DYCORS, the computationally expensive GSFLOW model can be efficiently incorporated into the simulation-optimization (SO) framework, and provide informative optimization results as it comprehensively simulates the basin-scale water cycle. Second, the optimization results demonstrate a very different time schedule of water diversion in opposite to the one existing in HRB, and manifest that, in areas where groundwater plays an important role in the hydrological cycle, water resources management must fully account for SW–GW interactions. Third, the temporal optimization suggests a basin-scale water saving through reduction of non-beneficial ET. As the integrated modeling revealed, the potential water saving can be achieved by "re-routing" the streamflow via an underground "aqueduct" (i.e., flow path), which represents a typical depletion-and-capture process. Finally, the results show that the current flow regulation would not be sustainable, since it essentially transforms the human-nature conflict between the middle HRB and the lower HRB into the one inside the middle HRB.

The above findings are important to hydrological modeling and water resources management in arid and semi-arid areas with intensive agriculture. Nevertheless, this study formulated a relatively simple optimization problem in which water quantity is the only concern. Future studies may consider other important factors including water quality, ecological stress, engineering feasibility, economic cost, etc., and address the optimization in a multi-objective framework.

Acknowledgements

This work was supported by the National Natural Science Foundation of China (NSFC) (No. 91225301; No. 91125021; No. 91425303). The data set was provided by Cold and Arid Regions Science Data Center in Lanzhou, China (http://westdc.westgis.ac.cn). The authors also extend great gratitude to Dr. Juliane Mueller and Christine A. Shoemaker for providing us the MATLAB code of DYCORS (Version 1.3).

References

Arnold, J.G., Kiniry, J.R., Srinivasan, R., Williams, J.R., Haney, E.B., Neitsch, S.L., 2011. Soil and Water Assessment Tool Input/Output File Documentation Version 2009. Texas Water Resources Institute Technical Report No. 365.
Baú, D.A., Mayer, A.S., 2006. Stochastic management of pump-and-treat strategies using surrogate functions. Adv. Water Resour. 29, 1901–1917.
Bhattacharjya, R.K., Datta, B., 2005. Optimal management of coastal aquifers using linked simulation optimization approach. Water Resour. Manag. 19, 295–320.
Bouwer, H., 2002. Integrated water management for the 21st Century: problems and solutions. J. Irrig. Drain. Eng. 128, 193–202.
Brunner, P., Simmons, C.T., 2012. HydroGeoSphere: a fully integrated, physically based hydrological model. Ground Water 50, 170–176.
Cai, X., Zeng, R., Kang, W.H., Song, J., Valocchi, A.J., 2015. Strategic Planning for Drought Mitigation under Climate Change. J. Water Resour. Plann. Manag., 04015004.
Castelletti, A., Galelli, S., Ratto, M., Soncini-Sessa, R., Young, P.C., 2012. A general framework for Dynamic Emulation Modelling in environmental problems. Environ. Modell. Software 34, 5–18.
Chang, L.C., Ho, C.C., Yeh, M.S., Yang, C.C., 2010. An Integrating approach for conjunctive-use planning of surface and subsurface water system. Water Resour. Manag. 25, 59–78.
Chen, Y., Zhang, D., Sun, Y., Liu, X., Wang, N., Savenije, H.H.G., 2005. Water demand management: A case study of the Heihe River Basin in China. Phys. Chem Earth, Parts A/B/C 30, 408–419.
Clerc, M., Kennedy, J., 2002. The particle swarm — explosion, stability, and convergence in a multidimensional complex space. IEEE Trans, Evol. Comput. 6, 58–73.
Cosgrove, D.M., Johnson, G.S., 2005. Aquifer management zones based on simulated surface-water response functions. J. Water Resour. Plann. Manag. 131, 89–100.
Deb, K., 2000. An efficient constraint handling method for genetic algorithms. Comput. Methods Appl. Mech. Eng. 186, 311–338.
Duan, Q.Y., Sorooshian, S., Gupta, V., 1992. Effective and efficient global optimization for conceptual rainfall-runoff models. Water Resour. Res. 28, 1015–1031.
Espinet, A., Shoemaker, C., Doughty, C., 2013. Estimation of plume distribution for carbon sequestration using parameter estimation with limited monitoring data. Water Resour. Res. 49, 4442–4464.
Forrester, A.I.J., Keane, A.J., 2009. Recent advances in surrogate-based optimization. Prog. Aerosp. Sci. 45, 50–79.
Galelli, S., Gandolfi, C., Soncini-Sessa, R., Agostani, D., 2010. Building a metamodel of an irrigation district distributed-parameter model. Agric. Water Manage. 97, 187–200.
Goldberg, D., 1989. Genetic Algorithms in Search, Optimization and Machine Learning. Addison-Wesley, Reading, Massachusetts, USA.
Graham, N., Refsgaard, A., 2001. MIKE SHE: A Distributed, Physically Based Modelling System for Surface Water/groundwater Interactions. Golden, Colorado.
Harbaugh, A.W., 2005. MODFLOW-2005 The U.S. Geological Survey modular ground-water model- the Ground-Water Flow Process. U.S. Geological Survey Techniques and Methods, pp. 6–A16.
Holland, J., 1975. Adap Tation in Natural and Artificial Systems. University of Michigan Press, Ann Arbor, Michigan, USA.
Ji, X., Kang, E., Chen, R., Zhao, W., Zhang, Z., Jin, B., 2006. The impact of the development of water resources on environment in arid inland river basins of Hexi region, Northwestern China. Environ. Geol. 50, 793–801.
Ji, X., Kang, E., Zhao, W., Chen, R., Xiao, S., Jin, B., 2005. Analysis on supply and demand of water resources and evaluation of the security of water resources in irrigation region of the middle reaches of Heihe River, Northwest China (in Chinese). Sci. Agric. Sin. 38, 9.
Johnson, V.M., Rogers, L.L., 2000. Accuracy of neural network approximators in simulation-optimization. J. Water Resour. Plann. Manag. 126, 48–56.
Khare, D., Jat, M.K., Ediwahyunan, 2006. Assessment of counjunctive use planning options: a case study of Sapon irrigation command area of Indonesia. J. Hydrol. 328, 764–777.
Kollet, S.J., Maxwell, R.M., 2006. Integrated surface–groundwater flow modeling: a free-surface overland flow boundary condition in a parallel groundwater flow model. Adv. Water Resour. 29, 945–958.
Krebs, J.R., Wilson, J.D., Bradbury, R.B., Siriwardena, G.M., 1999. The second silent spring? Nature 400, 611–612.
Kumar, S., Pavelic, P., George, B., Venugopal, K., Nawarathna, B., 2013. Integrated modeling framework to evaluate conjunctive use options in a canal irrigated area. J. Irrig. Drain. Eng. 139, 766–774.
Konikow, L.F., Leake, S.A., 2014. Depletion and capture: revisiting the source of water derived from wells. Ground Water 52, 100–111.
Leavesley, G.H., Lichty, R.W., Troutman, B.M., Saindon, L.G., 1983. Precipita Tion-runoff Modeling System-user's Manual. U.S. Geological Survey Water-Resources Investigations Report.
Li, F.-F., Shoemaker, C.A., Qiu, J., Wei, J.-H., 2015. Hierarchical multi-reservoir optimization modeling for real-world complexity with application to the Three Gorges system. Environ. Modell. Software 69, 319–329.
Liong, S., Khu, S., Chan, W., 2001. Derivation of pareto front with genetic algorithm and neural network. Derivation Pareto Front Genet. Algorithm Neural Network 6, 10.
Liu, L., Luo, Y., He, C., Lai, J., Li, X., 2010. Roles of the combined irrigation, drainage, and storage of the canal network in improving water reuse in the irrigation districts along the lower Yellow River, China. J. Hydrol. 391, 157–174.
Liu, X., Wang, L., 2012. Discussion on the scheduling scheme and water allocation curve of Heihe River (In Chinese). Gansu Water Resour. Hydropower Technol. 48, 3.
Mantoglou, A., Papantoniou, M., 2008. Optimal design of pumping networks in coastal aquifers using sharp interface models. J. Hydrol. 361, 52–63.
Markstrom, S.L., Niswonger, R.S., Regan, D.E., Prudic, P.M.B., 2008. Gsflow-coupled Ground-water and Surface-water Flow Model Based on the Integration of the Precipitation-Runoff Modeling System (PRMS) and the Modular Ground-Water Flow Model (MODFLOW-2005). U.S. Geological Survey Techniques and Methods.
McPhee, J., Yeh, W.W.G., 2008. Groundwater management using model reduction via empirical orthogonal functions. J. Water Resour. Plann. Manag. 134, 161–170.
Michael, L.M., Leonard, F.K., 2000. D Ocumentation of a Computer Program to Simulate Lake-aquifer Interaction Using the Modflow Ground-water Flow Model and the Moc3d Solute-transport Model. U.S. Geological water-resources investigations report.
Mugunthan, P., Shoemaker, C.A., 2006. Assessing the impacts of parameter uncertainty for computationally expensive groundwater models. Water Resour. Res. 42, W10428.
Niu, Z., Zhao, W., Huang, W., Chen, X., 2011. Impact of ecological water diversion on temporal and spatial change of water resources in Heihe Downstream (in Chinese). Hydrology 31, 5.
Ostfeld, A., Salomons, S., 2005. A hybrid genetic-instance based learning algorithm for CE-QUAL-W2 calibration. J. Hydrol. 310, 122–142.

Please cite this article in press as: Wu, X., et al., Optimizing conjunctive use of surface water and groundwater for irrigation to address human-nature water conflicts: A surrogate modeling approach. Agric. Water Manage. (2015), http://dx.doi.org/10.1016/j.agwat.2015.08.022

Pasetto, D., Guadagnini, A., Putti, M., 2011. POD-based Monte Carlo approach for the solution of regional scale groundwater flow driven by randomly distributed recharge. Adv. Water Resour. 34, 1450–1463.
Powell, M.J.D., 1992. The theory of radial basis function approximation in 1990, Advances in Numecal Analysis II: Wavelets, Subdivision, and Radial Basis Functions. Oxford University Press, Oxford, pp. 105–210.
Prasad, A.S., Umamahesh, N.V., Viswanath, G.K., 2006. Optimal irrigation planning under water scarcity. J. Irrig. Drain. Eng. 132, 228–237.
Razavi, S., Tolson, B.A., Burn, D.H., 2012. Review of surrogate modeling in water resources. Water Resour. Res. 48, W07401.
Regis, R.G., Shoemaker, C.A., 2007. A stochastic radial basis function method for the global optimization of expensive functions. INFORMS J. Comput. 19, 497–509.
Regis, R.G., Shoemaker, C.A., 2009. Parallel stochastic global optimization using radial basis functions. INFORMS J. Compu. 21, 411–426.
Regis, R.G., Shoemaker, C.A., 2013. Combining radial basis function surrogates and dynamic coordinate search in high-dimensional expensive black-box optimization. Eng. Optim. 45, 529–555.
Reichard, E.G., Johnson, T.A., 2005. Assessment of regional management strategies for controlling seawater intrusion. J. Water Resour. Plann. Manag. 131, 280–291.
Richard, G.N., David, E., Prudic, R.S.R., 2006. Documentation of the Unsaturated-Zone Flow (UZF1) Package for Modeling Unsaturated Flow Between the Land Surface and the Water Table with MODFLOW-2005. U.S. Geological Survey Techniques and Methods, pp. 6–A19.
Richard, G.N., David, E.P., 2010. Documentation of the Streamflow-Routing (SFR2) Package to Include Unsaturated Flow Beneath Streams-A Modification to SFR1. U.S. Geological Survey Techniques and Methods, pp. 6–A13.
Safavi, H.R., Esmikhani, M., 2013. Conjunctive use of surface water and groundwater: application of support vector machines (SVMs) and genetic algorithms. Water Resour. Manag. 27, 2623–2644.
Simons, G.W.H., Bastiaanssen, W.G.M., Immerzeel, W.W., 2015. Water reuse in river basins with multiple users: a literature review. J. Hydrol. 522, 558–571.
Singh, A., 2014a. Conjunctive use of water resources for sustainable irrigated agriculture. J. Hydrol. 519, 1688–1697.
Singh, A., 2014b. Simulation—optimization modeling for conjunctive water use management. Agric. Water Manag. 141, 23–29.
Singh, A., Panda, S.N., 2012. Development and application of an optimization model for the maximization of net agricultural return. Agric. Water Manag. 115, 267–275.
Singh, A., Panda, S.N., 2013. Optimization and simulation modelling for managing the problems of water resources. Water Resour. Manag. 27, 3421–3431.
Smout, I.K., Gorantiwar, S.D., 2005. Multilevel approach for optimizing land and water resources and irrigation deliveries for tertiary units in large irrigation Schemes. I: method. J. Irrig. Drain. Engineering 131, 254–263.
Tabari, M.M.R., Soltani, J., 2012. Multi-objective optimal model for conjunctive use management using SGAs and NSGA-II Models. Water Resour. Manag. 27, 37–53.
Tan, Q., Huang, G.H., Cai, Y.P., 2011. Radial interval chance-constrained programming for agricultural non-point source water pollution control under uncertainty. Agric. Water Manag. 98, 1595–1606.
Theis, 1940. The source of water derived from wells: essential factors controling the response of aquifers to development. Civil Eng. 10, 8.
Tian, Y., Zheng, Y., Wu, B., Wu, X., Liu, J., Zheng, C., 2015. Modeling surface water-groundwater interaction in arid and semi-arid regions with intensive agriculture. Environ. Modell. Software 63, 170–184.
Tolson, B.A., Shoemaker, C.A., 2007. Dynamically dimensioned search algorithm for computationally efficient watershed model calibration. Water Resour. Res. 43, W01413.
Wang, X., Yang, H., Shi, M., Zhou, D., Zhang, Z., 2015. Managing stakeholders' conflicts for water reallocation from agriculture to industry in the Heihe River Basin in Northwest China. Sci. Total Environ. 505, 823–832.
Weill, S., Mazzia, A., Putti, M., Paniconi, C., 2011. Coupling water flow and solute transport into a physically-based surface–subsurface hydrological model. Adv. Water Resour. 34, 128–136.
Wichelns, D., Oster, J.D., 2006. Sustainable irrigation is necessary and achievable, but direct costs and environmental impacts can be substantial. Agric. Water Manag. 86, 114–127.
Wu, B., Zheng, Y., Tian, Y., Wu, X., Yao, Y., Han, F., Liu, J., Zheng, C., 2014. Systematic assessment of the uncertainty in integrated surface water-groundwater modeling based on the probabilistic collocation method. Water Resour. Res. 50, 5848–5865.
Wu, B., Zheng, Y., Wu, X., Tian, Y., Han, F., Liu, J., Zheng, C., 2015. Optimizing water resources management in large river basins with integrated surface water-groundwater modeling: a surrogate-based approach. Water Resour. Res. 51, 2153–2173.
Zeng, X., Kang, S., Li, F., Zhang, L., Guo, P., 2010. Fuzzy multi-objective linear programming applying to crop area planning. Agric. Water Manag. 98, 134–142.
Zheng, Y., Wang, W., Han, F., Ping, J., 2011. Uncertainty assessment for watershed water quality modeling: a probabilistic collocation method based approach. Adv. Water Resour. 34, 887–898.

Please cite this article in press as: Wu, X., et al., Optimizing conjunctive use of surface water and groundwater for irrigation to address human-nature water conflicts: A surrogate modeling approach. Agric. Water Manage. (2015), http://dx.doi.org/10.1016/j.agwat.2015.08.022